Pielak, G. J., Atkinson, R. A., Boyd, J., & Williams, R. J. P. (1988b) *Eur. J. Biochem. 177*, 179–185.
Rance, M., Sorensen, O. W., Bodenhausen, G., Wagner, G., Ernst, R. R., & Wüthrich, K. (1984) *Biochim. Biophys. Acta 117*, 479–485.
Senn, H., Keller, R. M., & Wüthrich, K. (1980) *Biochem. Biophys. Res. Commun. 92*, 1362–1369.
Sklenar, V., & Bax, A. (1987) *J. Magn. Reson. 74*, 469–479.
Timkovich, R. (1979) in *The Porphyrins* (Dolphin, D., Ed.) pp 241–294, Academic Press, New York.
Timkovich, R. (1986) *Biochemistry 25*, 1089–1093.
Timkovich, R., Dhesi, R., Martinkus, K. M., Robinson, M. K., & Rea, T. (1982) *Arch. Biochem. Biophys. 215*, 45–58.
Timkovich, R., Cai, M. L., & Dixon, D. W. (1988) *Biochem. Biophys. Res. Commun. 150*, 1044–1050.
Wand, A. J., DiStefano, D. L., Feng, Y., Roder, H., & Englander, S. W. (1989) *Biochemistry 28*, 186–194.
Wüthrich, K. (1986) *NMR of Proteins and Nucleic Acids*, pp 40–202, Wiley-Interscience, New York.
Wüthrich, K., & Wagner, G. (1975) *FEBS Lett. 50* 265–268.

Resonance Raman Studies of Hemoglobins Reconstituted with Mesoheme. Unperturbed Iron–Histidine Stretching Frequencies in a Functionally Altered Hemoglobin†

Shanthini Jeyarajah and James R. Kincaid*
Chemistry Department, Marquette University, Milwaukee, Wisconsin 53233
Received December 8, 1989; Revised Manuscript Received February 16, 1990

ABSTRACT: Hybrid hemoglobins, containing mesoheme in one type of subunit and protoheme in the partner subunits, have been studied by resonance Raman spectroscopy. These hybrids have been studied in both the met hybrid and fully reduced, deoxy forms. Judicious choice of laser excitation frequency permits selective enhancement of modes associated with each type of subunit; i.e., either meso- or protoheme-containing subunit. The assignments of low-frequency modes of meso- and protoheme are briefly discussed with special reference to the iron–histidine linkage. Despite functional differences between the hybrids, no significant changes in the strength of the iron–histidine linkages are detected by resonance Raman spectroscopy. These results are discussed with reference to recent high-resolution NMR studies of these same hybrids.

The mechanism of hemoglobin (Hb) cooperativity continues to occupy a prominent position as a subject of interest in biophysical research (Antonini et al., 1981; Baldwin, 1975; Ackers & Smith, 1987). Despite a considerable effort by many research groups and an impressive history of accomplishment, precise definition of the stereochemical mechanisms by which ligand binding to one subunit affects the reactivity of the partner subunits remains elusive. In addition to structural and functional characterization of the native protein, the characterization of biologically (i.e., mutant) and chemically modified derivatives represents a useful approach to investigate these mechanisms (Imai, 1985; Pettigrew et al., 1982; Simolo et al., 1985). Specific interactions of the prosthetic group (heme) substituents with surrounding protein residues has not been overlooked (Sono & Asakura, 1974; Seybert et al., 1976; Chang et al., 1984; Kawabe et al., 1982; Makino & Sugita, 1978). In fact, elegant calculations carried out by Karplus and co-workers support convincing arguments for the importance of specific substituent–residue interactions (Gelin et al., 1983). Thus, hemoglobin has been reconstituted with a variety of hemes bearing a number of different substituents and the functional properties of these derivatives have been carefully documented. While such functional characterization studies are essential for establishing the effectiveness of a particular chemical modification in altering ligand-binding properties, it is important to document modification-induced perturbations in structure and bonding at key sites within the tetramer in order to gain insight into the structural basis for the effect. It is only relatively recently that sophisticated structural probes of the heme and its surroundings have been developed, two of the most powerful of which are nuclear magnetic resonance (NMR) (Lamar, 1979; Ho & Russu, 1981) and resonance Raman (RR) spectroscopies (Kitagawa, 1986; Spiro, 1985; Rousseau & Friedman, 1988; Yu, 1986).

Thus far, only one report has appeared in which NMR was used to provide complementary active-site structural characterization of a hemoglobin derivative containing a selectively modified heme. Thus, Ishimori and Morishima (1986) have described thorough NMR spectroscopic studies of deuteroheme and mesoheme derivatives of Hb; i.e., $(\alpha_m\beta_p)_2$, $(\alpha_p\beta_m)_2$, $(\alpha_m\beta_m)_2$, and $(\alpha_d\beta_d)_2$ [where the d and m subscripts designate a deuteroheme- or mesoheme-containing subunit and the p subscript indicates that the subunit contains the (native) protoheme prosthetic group].

In this report we present results of corresponding RR studies of mesoheme-reconstituted Hb derivatives as the deoxy tetramers and metcyano hybrids. Judicious choice of laser excitation wavelength permits selective enhancement of the individual subunits in the fully deoxy hybrids and reveals iron–histidine stretching frequencies that are not substantially different from those of the native system.

Experimental Procedures

Preparation of Hb Derivatives. Mesohemin chloride was purchased from Mid Century Chemical Co., Posen, IL, and used as received. All samples were found to be pure as determined by pyridine hemochromogen spectra (Smith, 1975) and thin-layer chromatography (DiNello & Dolphin, 1975) (single spot).

† This work was supported by a grant from the National Institutes of Health (DK 35153 to J.R.K.).

0006-2960/90/0429-5087$02.50/0

Hb was isolated from washed red blood cells (obtained from a local blood center) according to literature procedures (Riggs, 1981). The experimental conditions described here are for working with ~10 g of hemoglobin in a volume of 100 mL. Hemoglobin was dissociated into its subunits by reaction of $(\alpha^{CO}\beta^{CO})_2$ with *p*-(chloromercuri)benzoate (PMB), as described by Yip et al. (1977).

Rather than use the two-column procedure to isolate the subunits (i.e., discarding 50% of the protein) as described in the earlier work, after centrifugation to remove precipitates, the PMB–Hb solution was equilibrated with 50 mM tris(hydroxymethyl)aminomethane hydrochloride (Tris-HCl) buffer, pH 8.4, by filtration through a Bio-Gel P-6 column (5 × 50 cm). The eluent was then applied to a (diethylaminoethyl)-(DEAE) cellulose (Whatman DE-52) column (5 × 10 cm) equilibrated with the same buffer. The (electrophoretically pure) α-PMB subunits are first eluted with this buffer and are followed by a well-separated band of unreacted hemoglobin tetramer. The β-PMB subunits were retained on the DEAE column under these conditions. Another buffer, 0.1 M phosphate, pH 7.4, was then applied to the DEAE column to elute the (electrophoretically pure) β-PMB. The α^{CO} and β^{CO} forms were regenerated from the α^{CO}_{PMB} and β^{CO}_{PMB} as was described (Yip et al., 1977) and the purity of the isolated subunits was checked by polyacrylamide gel electrophoresis according to the procedure described by Riggs (1981).

Apoglobin chains were prepared via the acid–acetone procedure described previously (Yip et al., 1972) using the carbon monoxide derivative as the starting material. The resulting (white) globin precipitate was dissolved in a minimum amount (200 mg of globin in 10 mL) of cold distilled water. The aposubunit solution was first dialyzed against distilled water for 0.5 h to remove the remaining acetone. The globin solution was then dialyzed for 2 h against pH 6.4 20 mM Bis-Tris buffer [2,2-bis(hydroxymethyl)-2,2′,2″-nitrilotriethanol] for α subunits or against pH 5.7 20 mM Bis-Tris buffer for β subunits. It is found that the above dialysis procedures prevented the precipitation of the aposubunits that occurs when phosphate buffer is used. The typical yield of this process from carboxy subunit to aposubunit is 95% (based on UV absorbance measurements).

For reconstitution of the apoglobins, 3 mg of mesohemin was dissolved initially in a minimum volume of 0.1 M KOH (~1 mL) and then diluted to a final volume of 10 mL. This was done immediately before the recombination procedure. Both ultraviolet and visible spectra of globin were taken after dialysis (Perkin-Elmer 320 spectrophotometer). The α- and β-globins have a strong absorbance at 280 nm with a molar absorptivity of 1×10^4 for α and 1.54×10^4 for β chains (Yip et al., 1972). The concentration of the hemin solution was determined spectrophotometrically by using the value of 5.0×10^4 as the molar absorptivity at 385 nm (Gibson & Antonini, 1963). A 1.2 molar excess of hemin was added dropwise into a gently stirred globin solution immersed in an ice bath. During the addition, the pH of the α chain was monitored and maintained in a range of 6.2–6.4 by adding 10 mM HCl. For the β subunit the pH was maintained at 5.7. The optimum pH ranges for these reconstitution procedures were determined by comparing the yields for several pH values for each subunit. The resulting mixture was then allowed to stir for 5 min, was saturated with N_2, and was then allowed to stand in the refrigerator overnight. Excess hemin is readily removed by chromatography on a Sephadex G-25 column (2.5 × 40 cm) equilibrated with 20 mM phosphate buffer, pH 6.4. Following chromatography, the subunit was converted to the metcyanide derivative by addition of (excess) KCN and rechromatographed on the Sephadex G-25 column to remove the excess KCN. Small amounts of protein are lost during each of these steps, with the typical yield of the metcyanide derivative (from the aposubunit) being 75%.

The met hybrid derivatives were prepared by combining an equal amount of the CO form of the complementary subunit with metcyanide derivatives of the modified subunit. The resulting mixture was allowed to stand at 4 °C overnight to ensure the formation of the tetramer. The recombined sample was equilibrated with 20 mM phosphate buffer, pH 6.4, on a Bio-Gel P-6 column (2.5 × 40 cm) and then loaded onto a CM-cellulose column (2.5 × 4 cm) equilibrated with the same buffer. After unreacted β subunit was washed out with this buffer, the reconstituted Hb was eluted with 30 mM phosphate buffer, pH 7.0. The unreacted α subunit does not migrate with this buffer. The yield of this procedure from met reconstituted subunit to hybrid Hb is ~60%.

The met hybrid solution was applied to Bio-Gel P-6 column (2.5 × 40 cm) equilibrated with the appropriate buffer (50 mM Bis-Tris, pH 6.4, or 50 mM Tris, pH 9.0) (i.e., the buffer used for the spectral measurements). The Hb (in the CO ligated form) was converted to the oxy form by photodissociation of CO in the presence of oxygen. In order to convert the oxy subunit to the deoxy form, the sample of the modified hybrid hemoglobin was deoxygenated by repeated evacuation and flushing with pure nitrogen gas. Three times were usually adequate. Inositol hexaphosphate (IHP) was purchased from Aldrich Chemical Co. Solid IHP was first dissolved in 50 mM Bis-Tris buffer and titrated to pH 6.4 with HCl. The IHP solution was added in a molar ratio of 5:1 to the reconstituted hemoglobin samples under anaerobic conditions.

The deoxy forms of the separated subunits α_m and β_m were prepared by reducing the metcyano subunits with sodium dithionite under a nitrogen atmosphere. The hybrids, $(\alpha_p\beta_m)_2$ and $(\alpha_m\beta_p)_2$, were prepared by reducing the met hybrids $(\alpha_p\beta^{CN}_m)_2$ and $(\alpha_m\beta^{CN}_p)_2$, with sodium dithionite under a CO atmosphere.

The excess dithionite was removed by passing through a Bio-Gel column equilibrated with a 50 mM phosphate buffer, pH 7.0. The CO forms of the hybrids were converted to the deoxy forms as described above. A few crystals of sodium dithionite were added to the sample under anaerobic conditions after the deoxygenation.

Raman Spectral Measurements. Resonance Raman spectra were obtained by using a Spex Model 1403 spectrometer equipped with a Model DM1B spectroscopy laboratory coordinator. The 441.6-nm excitation line of a helium:cadmium laser (Liconix Model 4240NB) was employed for excitation of all samples with the protoheme deoxy form (deoxyprotoheme has a Soret band at 430 nm). The 406.7-nm excitation line of a Coherent Innova 100 krypton ion laser was employed for excitation of all samples with the mesoheme deoxy form (deoxymesoheme has the Soret band at 421 nm). Throughout the measurements at room temperature the Raman cell was spun to lessen local heating of the protein solution. Typical concentrations ranged from 0.04 to 0.1 mM in heme. All spectra were calibrated by scanning over the Rayleigh line with low collection efficiency. For both sets of spectral measurements the spectral slit width was maintained at 2–5 cm^{-1} (corresponding to a mechanical slit width of 150–300 μm). Reported wave numbers are accurate to ±1 cm^{-1}.

Results and Discussion

A. Assignments of Low-Frequency Modes. The low-frequency RR spectra of mesoHb and its isolated subunits are

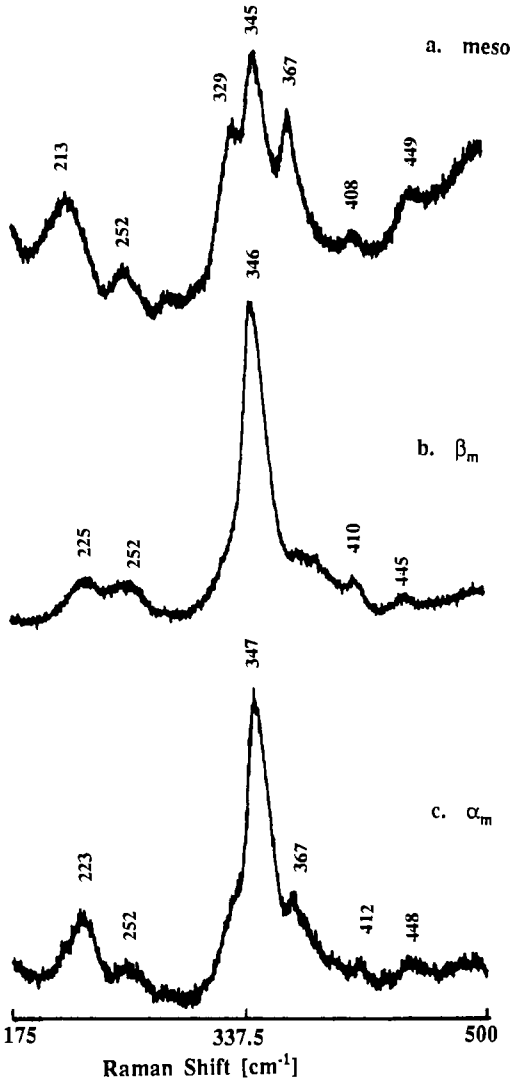

FIGURE 1: Low-frequency resonance Raman spectra of (a) deoxy-mesoHb, (b) deoxy-β_m subunit, (c) deoxy-α_m subunit; 100 mM, pH 7.0, 406.7-nm excitation.

given in Figure 1. For comparison purposes, corresponding spectra of the native system are shown in Figure 2. The latter are in agreement with those previously reported (Nagai et al., 1980; Ondrias et al., 1982). The frequencies of all systems studied in this work are summarized in Table I.

Briefly, the low-frequency spectra of these deoxyheme proteins contain both in-plane and out-of-plane modes associated with the porphyrin macrocycle and its substituents as well as the iron–histidyl–imidazole mode, designated as ν(Fe–N_ϵ). The assignment of this latter mode to the feature located near 220 cm^{-1} in Figures 1 and 2 has now been unambiguously confirmed by ^{54}Fe/^{56}Fe and ^{14}N/^{15}N (heme macrocycle) isotopic substitution (Nagai et al., 1980; Kitagawa et al., 1979; Argade et al., 1984). This important feature is expected to be sensitive to tertiary and quaternary structural changes and solution conditions and has in fact been observed to occur over a relatively large range of frequencies (i.e., 201–232 cm^{-1}) in different hemoglobin and myoglobin derivatives under various conditions (Rousseau & Friedman, 1988).

It is somewhat difficult to clearly describe the other low-frequency bands inasmuch as they are associated with complex motions of the heme macrocycle and its substituents. Recently, it has become evident that the position and intensities of these modes are sensitive to peripheral substituent orientation (Brennan et al., 1988; Li et al., 1989). While such behavior

Table I: Low-Frequency Modes (ν, cm^{-1}) of Separated Chains and Native, Modified, and Hybrid Hemoglobins

HbA	α_p	$\alpha_p\beta_p^{CN}$	$\alpha_p\beta_p^{CN}$ + IHP	$\alpha_p\beta_m^{CN}$	$\alpha_p\beta_m^{CN}$ + IHP	$(\alpha_p\beta_m)_2$	β_p	$\alpha_p^{CN}\beta_p$	$\alpha_p^{CN}\beta_p$ + IHP	$\alpha_m^{CN}\beta_p$	$^{CN}_m\beta_p$ + IHP	$(\alpha_m\beta_p)_2$	α_m	$(\alpha_m\beta_p)_2$	β_m	$(\alpha_p\beta_m)_2$	meso-Hb	assignment
215	223	223	201/212	223	201/213	206	224	223	219	222	218	216	223	206	225	219	213	ν(Fe–N_ϵ)
302	302	301	302	302	302	301	302	302	302	301	301	302						γ($C_aC_{m(A_{2u})}$)
													329				329	
342	342	342	343	343	343	342	342	343	342	342	343	342	347	344	346	341	345	$\nu_{8(A_{1g})}$
366	365	366	366	366	366	366	366	367	367	367	367	365	367	366		366	367	$\delta C_6S_{(A_{2u})}$
405	405	405	406	405	405	405	406	406	406	406	406	406	412	408	410	407	408	$\delta C_bC_aC_\beta$
433	430	430	430		433	430							448	449	445		449	

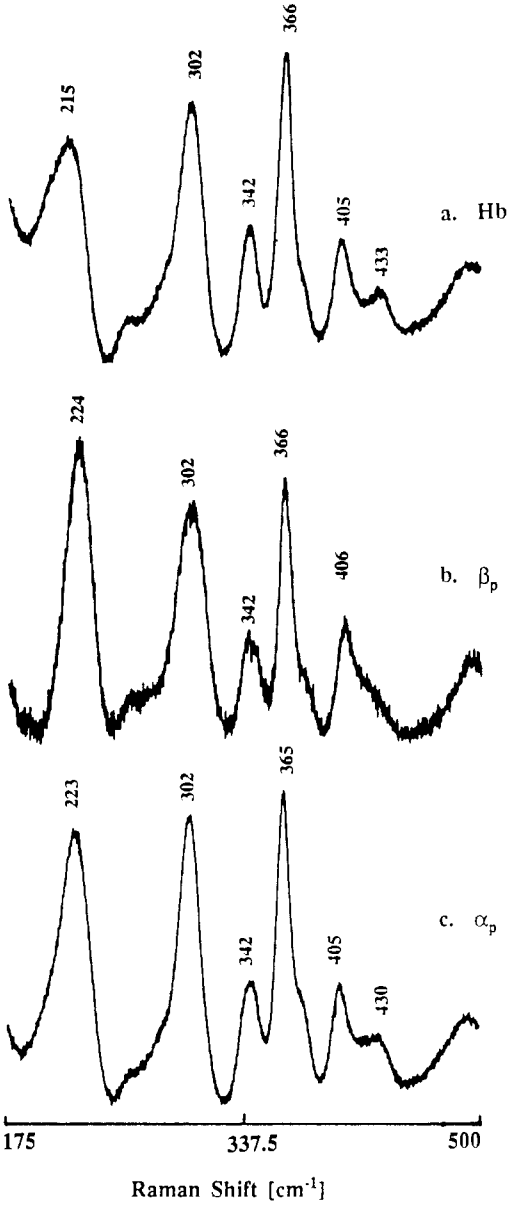

FIGURE 2: Low-frequency resonance Raman spectra of (a) deoxyHbA, (b) deoxy-β_p subunit, (c) deoxy-α_p subunit; pH 6.5–7.0, 441.6-nm excitation.

offers promise as a powerful structural probe of substituent–protein interactions, it will require extensive work to establish a reliable interpretive framework. However, although further work is needed to definitively assign these other low-frequency modes, some progress has been made for the native system by using selectively deuteriated protohemes and nickel protoporphyrin (Lee et al., 1986; Choi & Spiro, 1983; Desbois et al., 1984).

The relatively strong feature located at 367 cm^{-1} has been assigned to an out-of-plane deformation of peripheral substituents coupled with a lower frequency tilting of the pyrrole rings (Choi & Spiro, 1983). While a feature observed near 375 cm^{-1} in the spectrum of selectively deuteriated nickel protoporphyrin 1X dimethyl ester has been assigned to the first overtone of a lower frequency depolarized mode (i.e., $2\nu_{35}$) (Lee et al., 1986), it is not likely that the relatively intense 367-cm^{-1} feature observed in the spectra of the deoxyheme proteins can be properly correlated with this overtone.

The feature located at ~345 cm^{-1} has been correlated with the (in-plane) ν_8 (A_{1g}) mode of the highly symmetrical NiOEP and apparently contains major contributions from in-plane deformation of the peripheral substituents. Based on its behavior upon selective deuteriation of ring methyl substituents, it probably involves motions of the substituents at rings three and four (Lee et al., 1986). An interesting discussion of the behavior of this mode in photolysed transients and at low temperature has been presented by Rosseau and Friedman (1988).

The remaining prominent feature, located at 301 cm^{-1}, has previously been assigned to an out-of-plane (in-phase) deformation of methine carbons [i.e., $\gamma(C_m)$] based on an observed 7-cm^{-1} shift to lower frequency upon deuteriation of the methine positions (Choi et al., 1983). The weak features located at 405 and 435 cm^{-1} are associated with vinyl group deformations (Lee et al., 1986; Uchida et al., 1988). The spectra of the corresponding mesoheme-containing species (Figure 1) are much less complex. Those of the isolated subunits (traces b and c) exhibit a prominent feature (ν_8) at 347 cm^{-1} as well as ν(Fe–N_ϵ) at ~225 cm^{-1}, but other modes appearing at ~411, 365, and 252 cm^{-1} are extremely weak. As will be discussed later, the most notable difference between the native system and the mesoheme analogues is the dramatic alteration of intensities that occurs in the case of tetrameric mesoHb. No such change occurs in the case of the native system; i.e., the frequencies and relative intensities of the bands at 302, 345, 367, 406, and 411 cm^{-1} are virtually identical in traces a–c of Figure 2.

B. Effects of Substituents on ν(Fe–N_ϵ). 1. Valency Hybrids. As is seen in Figure 2, the ν(Fe–N_ϵ) is observed at ~225 cm^{-1} in the spectra of the isolated subunits but broadens and shifts down to ~215 cm^{-1} in the spectrum of the (T-state) tetramer. This behavior has been nicely clarified by Nagai and Kitagawa (1980) in their elegant study of the valency hybrids. While other workers have been unable to reproduce the data for the met hybrid systems owing to solution instability, they obtained similar results for the iron/cobalt hybrids (Ondrias et al., 1982). In order to confirm the data for the met hybrids, and to provide reference data for comparison with the mesoheme analogues, we have repeated the experiments with the native met hybrids. Our results, shown in Figure 3, are virtually identical with those reported by Nagai and Kitagawa (1980).

These valency hybrids are considered to exist in an "R-like" quaternary conformation but are switched to "T-like" state upon addition of IHP. Selective excitation of the ferrous subunits is achieved by using 442-nm excitation, so that the spectra shown in Figure 3 are associated with the ferrous subunits only. In traces c and d it is seen that the ν(Fe–N_ϵ) of the β subunit of R-$(\alpha_p^{CN}\beta_p)_2$ occurs at 223 cm^{-1} (a value which is similar to that observed for the isolated β subunit) but shifts down by 4 cm^{-1} to 219 cm^{-1} upon transition to T-$(\alpha_p^{CN}\beta_p)_2$. The corresponding data for the α subunit of $(\alpha_p\beta_p^{CN})_2$ are more complex (traces a and b). The R-$(\alpha_p\beta_p^{CN})_2$ exhibits a reasonably strong, symmetric feature at 223 cm^{-1} similar to those obtained for the isolated subunits and R-$(\alpha_p^{CN}\beta_p)_2$. However, upon addition of IHP, this feature actually splits into two features located at 201 and 212 cm^{-1}, implying both a substantial weakening of the iron–histidine linkage (relative to that observed for the β subunits) and a significant difference in the individual α subunits. A similar α-subunit heterogeneity was noted for the iron/cobalt hybrids (Ondrias et al., 1982). The other low-frequency protoheme modes are not sensitive to the R to T switch.

The spectra of the corresponding mesoheme analogues are given in Figure 4. In these cases the mesoheme subunits are oxidized (i.e., not probed) and the ferrous protoheme subunits

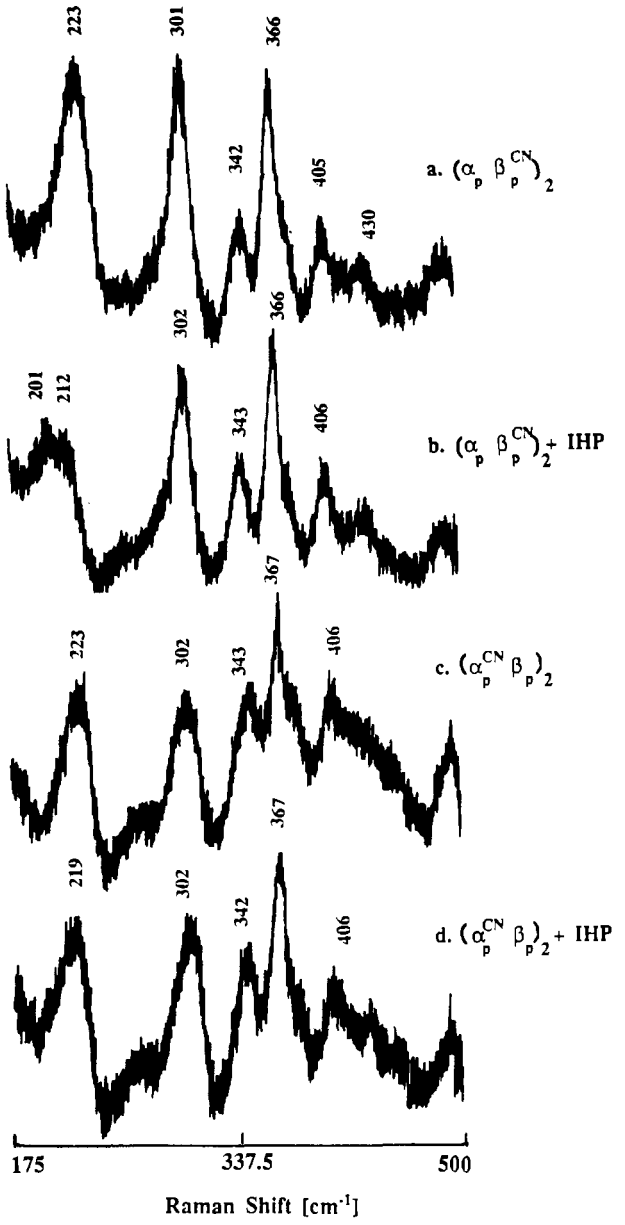

FIGURE 3: Low-frequency resonance Raman spectra of (a) deoxy-$(\alpha_p\beta_p^{CN})_2$, pH 9.0; (b) deoxy-$(\alpha_p\beta_p^{CN})_2$ + IHP, pH 6.5; (c) deoxy-$(\alpha_p^{CN}\beta_p)_2$, pH 9.0; (d) deoxy-$(\alpha_p^{CN}\beta_p)_2$ + IHP, pH 6.5; 441.6-nm excitation.

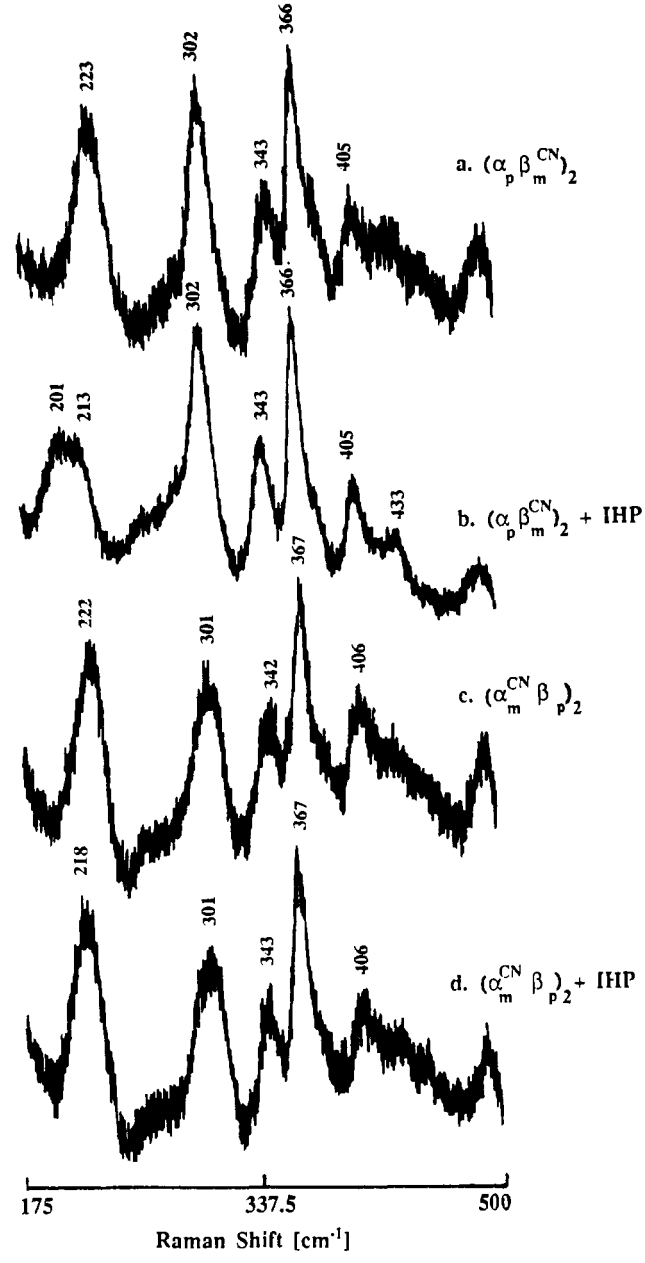

FIGURE 4: Low-frequency resonance Raman spectra of (a) deoxy-$(\alpha_p\beta_m^{CN})_2$, pH 9.0; (b) deoxy-$(\alpha_p\beta_m^{CN})_2$ + IHP, pH 6.5; (c) deoxy-$(\alpha_m^{CN}\beta_p)_2$, pH 9.0; (d) deoxy-$(\alpha_m^{CN}\beta_p)_2$ + IHP, pH 6.5; 441.6-nm excitation.

are examined. These experiments clearly demonstrate that heme substituent modification in one subunit has an insignificant effect on the protein–heme interactions in the partner subunit. Thus, the ferrous–protoheme subunits of both the R and T states of $(\alpha_p\beta_m^{CN})_2$ and $(\alpha_m^{CN}\beta_p)_2$ exhibit spectra that are essentially identical with those shown in Figure 3.

2. Deoxy Forms. Replacement of vinyl groups by ethyl groups causes an approximately 10-nm hypsochromic shift of the macrocycle π–π^* transitions. The Soret maximum of the deoxy derivative containing mesoheme is observed at 421 nm compared with 430 nm in the case of the (native) protoheme species (Kawabe et al., 1982; Sugita, 1975). The enhancement of the low-frequency modes, including ν(Fe–N_ϵ), has been shown to parallel the absorption spectrum (Bancharoenpaurpong et al., 1984). Thus, it is expected that the low-frequency protoheme modes will maximize near 430 nm while those associated with the mesoheme analogues will be most strongly enhanced near 420 nm. This relatively large separation of Soret maxima facilitates selective enhancement of individual subunits in the hybrids $(\alpha_m\beta_p)_2$ and $(\alpha_p\beta_m)_2$.

The RR spectra of these hybrids are given in Figure 5. In these experiments, the 441.6-nm line from a He:Cd laser was used to specifically enhance modes associated with the protoheme-containing subunits (traces b and d). In both cases, enhancement of modes associated with the mesoheme-containing subunit is not expected inasmuch as the excitation wavelength (441.6 nm) is relatively far removed (~20 nm) from the absorption maximum (~420 nm). Similarly, utilization of the 406.7-nm line (Kr^+ laser) selectively enhances the mesoheme modes.

The spectral data in Figure 5 and the data in Table I reveal the following behavior. In the case of the $(\alpha_p\beta_m)_2$ hybrid, the ν(Fe–N_ϵ) region for the (protoheme) α subunit (trace b) exhibits an asymmetric band at 206 cm^{-1} with components at 201 and 212 cm^{-1}. The appearance of this spectrum is quite similar to those of the $(\alpha_p\beta_p^{CN})_2$ and $(\alpha_p\beta_m^{CN})_2$ hybrids in the presence of IHP (Figures 3b and 4b). The ν(Fe–N_ϵ) of the β_p subunit in $(\alpha_m\beta_p)_2$ (Figure 5d) is only 1 or 2 cm^{-1} lower than its frequency for the corresponding valency hybrids in

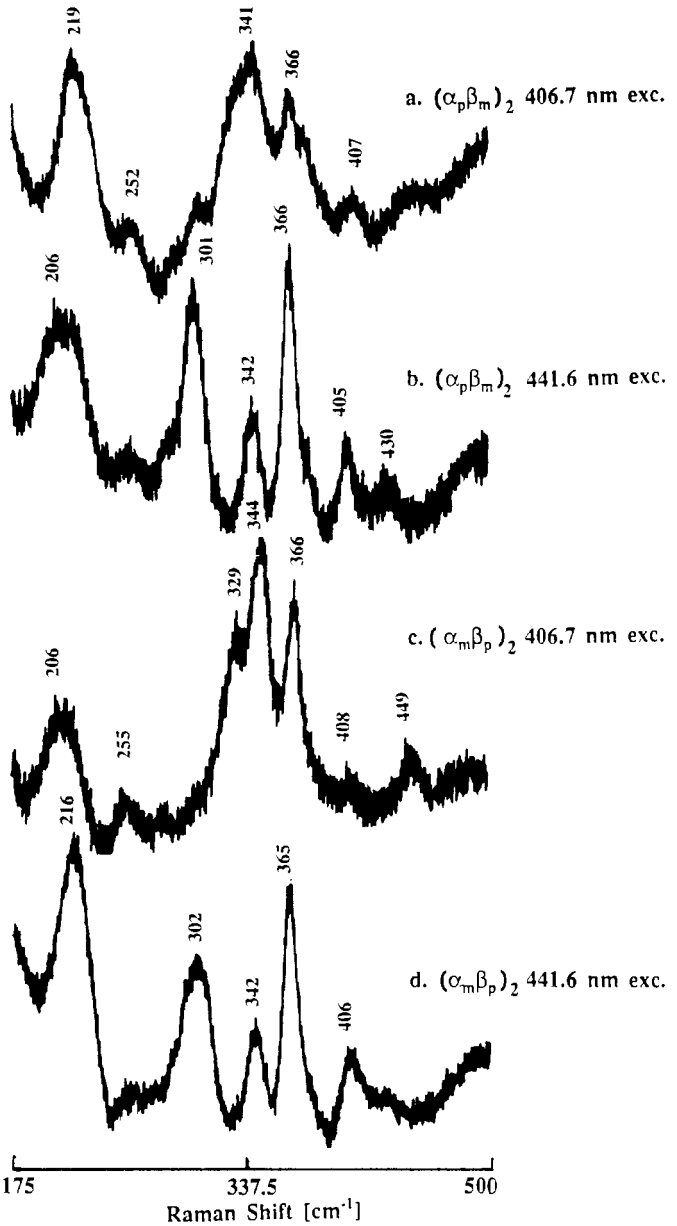

FIGURE 5: Low-frequency resonance Raman spectra of (a) $(\alpha_p\beta_m)_2$, 406.7-nm excitation; (b) $(\alpha_p\beta_m)_2$, 441.6-nm excitation; (c) $(\alpha_m\beta_p)_2$, 406.7-nm excitation; (d) $(\alpha_m\beta_p)_2$, 441.6-nm excitation, pH 7.0.

the presence of IHP (Figures 3d and 4d).

In both of these cases [i.e., α_p in $(\alpha_p\beta_m)_2$ and β_p in $(\alpha_m\beta_p)_2$], small or insignificant changes are detected in the frequency of ν(Fe–N_ϵ). While, these data may not be considered surprising (in view of the fact that only the hemes in the partner subunit are modified), the corresponding data for the mesoheme subunits is somewhat unexpected. Thus, in the case of α_m in $(\alpha_m\beta_p)_2$, the ν(Fe–N_ϵ) is again observed near 206 cm^{-1} with some indication of heterogeneity in the α subunits (Figure 5c). This behavior is therefore quite similar to the behavior of the α_p subunit in the met hybrids (with IHP present) and implies that substitution of ethyl groups for vinyl groups has little or no effect on the iron–histidine linkage. A similar implication is provided by the spectrum of β_m in $(\alpha_p\beta_m)_2$ (Figure 5a), where ν(Fe–N_ϵ) is observed at 219 cm^{-1}. This frequency is essentially identical with those obtained for β_p in $(\alpha_p^{CN}\beta_p)_2$ and $(\alpha_m^{CN}\beta_p)_2$ in the presence of IHP (Figures 3d and 4d). The other low-frequency modes of the mesoheme in the various derivatives are apparently quite sensitive to subtle structural differences in the heme pocket. In the isolated subunits (Figure 1), the band at 347 cm^{-1} dominates both spectra with weak features being observed at 252, 412, and 367 cm^{-1}, the last being more prominent in the spectrum of α_m (trace c). In the tetramer (trace a), a complex pattern appears near 350 cm^{-1} with components at 329, 345, and 367 cm^{-1}.

As can be seen in Figure 5, the α_m subunit in the hybrid tetramer (trace c) exhibits a spectrum essentially identical with that of mesohemoglobin (Figure 1a) with the exception of the ν(Fe–N_ϵ) region. The β_m subunit of the hybrid tetramer (trace a) exhibits a ν(Fe–N_ϵ) which is 6 cm^{-1} lower than that of isolated β_m (Figure 1b) and the features at 367 and (possibly) 329 cm^{-1} are slightly stronger relative to the intense band near 345 cm^{-1}.

Thus, in the case of mesoheme-containing species, the lowering of the ν(Fe–N_ϵ) appears to be accompanied by alterations in frequencies and/or intensities of other low-frequency heme modes. Furthermore, these other modes presumably (by analogy with protoheme assignments) contain substantial contributions from heme peripheral substituents. It is therefore unfortunate that a better description of these low-frequency modes is not available inasmuch as it may lead to a clearer understanding of the manner in which protein–substituent interactions can affect iron–histidine bonding. Further studies employing isotopically labeled mesoheme will be required to clarify the low-frequency spectral patterns.

In summary of this section, further work will be needed before the low-frequency spectra can be interpreted in terms of heme structural changes that accompany protein conformational changes. However, the ν(Fe–N_ϵ) modes are relatively isolated and can presumably be directly correlated with iron–histidine bond strength (Rosseau & Friedman, 1988). Perhaps not surprisingly, the present results show that heme substitution in one subunit has no effect on the iron–histidine linkage in the partner subunit. However, given the fact that oxygen-binding properties of the modified hybrids are altered (vide infra), it may seem unexpected that peripheral substituent modification at a given heme has a small or insignificant effect on the iron–histidine linkage; i.e., the ν(Fe–N_ϵ) of the α subunit of $(\alpha_p\beta_p)_2$ is quite similar to that of $(\alpha_m\beta_p)_2$ and essentially no frequency shift or broadening is observed for the β subunit of $(\alpha_p\beta_m)_2$ compared to $(\alpha_p\beta_p)_2$. However, it should be pointed out that recent work by Srajer et al. (1988) provides a detailed theoretical framework that can account for energy differences associated with variations in oxygen affinities in the absence of Raman frequency shifts.

Finally, it should be emphasized that the results reported here are relevant to the controversy concerning the relationship of the iron–imidazole frequency to oxygen affinity. While Kitagawa and co-workers (Matsukawa et al., (1985) had previously constructed a theory connecting these two parameters, more recent work indicates that the iron–imidazole frequency in hemoglobin does not correlate with affinity, but depends only on the quaternary structure and the subunit (Coppey et al., 1986). The results presented here provide clear-cut support for the latter view.

C. Relationship of RR Data to Other Structural and Functional Studies of Proto/Meso Hybrids. The oxygenation curves for these hybrids have been obtained and analyzed previously (Yammamoto et al., 1974). The $(\alpha_m\beta_p)_2$ hybrid exhibits a lowered cooperativity (n = 1.7) and relatively high oxygen affinity (P_{50} = 2.5 and 7.0 Torr for α_m and β_p, respectively), the corresponding values for native Hb being n = 2.5 (Note: We have cited Yamamoto's value although n is usually given as 2.8 for native Hb) and P_{50} = 13 Torr. The other hybrid, $(\alpha_p\beta_m)_2$ also exhibits lower cooperativity (n =

1.7) and a higher oxygen affinity (P_{50} = 3.3 Torr). As is the case for most mutant and modified hemoglobins, lowered cooperativity and increased oxygen affinity are presumed to be manifestations of a destabilized T state brought about by alteration of delicately balanced protein–protein or protein–heme interactions. Conversely, such modifications are usually considered to have little effect on the R-state properties. In the cases of the proto/meso hybrids some evidence in support of this assumption is available in the form of detailed NMR studies by Ishimori and Morishima, who obtained high-quality NMR spectra for deoxy- and oxygenated protoheme/mesoheme hybrids. These workers found that the spectra of the fully ligated tetramers exhibited characteristic R-state resonances, which were virtually identical with those observed for native oxygenated Hb. This was interpreted as evidence that, in the ligated derivatives, the substitution of mesoheme for protoheme in either subunit has no significant effect on the quaternary structure of the tetramer nor on the tertiary structures of the reconstituted or partner subunits.

On the other hand, the NMR studies of the nonligated derivatives do demonstrate an effect of substituent modification. The characteristic T-state "marker resonances" were monitored and the iron–histidine linkages were probed via observation of the hyperfine-shifted proximal imidazole $N_\delta H$ resonances. The essential conclusion of that work was that, based on an analysis of the resonances ascribed to intersubunit linkages, heme substituent modification alters the teriary structure of the modified subunit so as to generate an "imperfect T state". It was also noted that the substituent modification resulted in slight perturbations of the iron–imidazole linkages of the modified subunits but not those of the partner subunits. Finally, from an analysis of the magnitudes of the observed shifts, Ishimori and Morishima concluded that modification of the heme peripheral substituents of the β subunit has a more pronounced effect on the tertiary and quaternary structures of the protein than does modification of the α subunit.

It is useful to compare results of the RR studies with the NMR results. Whereas NMR spectroscopy detects alterations at the active site upon replacement of vinyl groups with ethyl groups, the RR spectra show no significant changes. For example, in the case of $(\alpha_p\beta_m)_2$, the $N_\delta H$ resonance of the β_m subunit is shifted compared to that of β_p of native Hb. In contrast, the $\nu(Fe–N_\epsilon)$ of β_m in $(\alpha_p\beta_m)_2$ is observed at 219 cm^{-1}, a frequency that is insignificantly different (219 vs 218 cm^{-1}) from the value observed for β_p in the T-state hybrids [$(\alpha_p^{CN}\beta_p)_2$ and $(\alpha_m^{CN}\beta_p)_2$ in the presence of IHP].

Apparently, the $N_\delta H$ NMR resonance is more sensitive to subtle active-site structural alterations than is the RR probe, $\nu(Fe–N_\epsilon)$. The latter is presumably an effective probe of the strength of the iron–histidine linkages whereas the former is determined by additional factors, e.g., hydrogen bonding to the peptide framework (Nagai et al., 1982) and slight changes in the actual nuclear positions (Srajer, et al., 1975).

References

Ackers, G. K., & Smith, F. R. (1987) *Annu. Rev. Biophy. Biophys. Chem. 16*, 583–609.

Antonini, E., Rossi-Bernardi, K., & Chiancone, E. (1981) *Methods Enzymol. 76*.

Argade, P. V., Sassaroli, M., Rosseu, D. L., Inubushi, T., Ikeda-Saito, M., & Lapidot, A. (1984) *J. Am. Chem. Soc. 106*, 6593–6596.

Baldwin, J. M. (1975) *Prog. Biophys. Mol. Biol. 29*, 225–320.

Bangcharoenpaurpong, O., Schomacher, K. T., & Champion, P. M. (1984) *J. Am. Chem. Soc. 106*, 5688–5698.

Brennan, J. D., Scheidt, W. R., & Shellnut, J. A. (1988) *J. Am. Chem. Soc. 110*, 3919–3924.

Chang, C. K., Ward, B., & Ebina, S. (1984) *Arch. Biochem. Biophys. 231*, 366–371.

Choi, S., & Spiro, T. G. (1983) *J. Am. Chem. Soc. 105*, 3683–3692.

Coppey, M., Dasgupta, S., & Spiro, T. G. (1986) *Biochemistry 25*, 1940–1944.

Debois, A., Henry, Y., & Lutz, M. (1984) *Biochim. Biophys. Acta 785*, 148–160.

DiNello, R. K., & Dolphin, D. (1975) *Anal. Biochem. 64*, 444–449.

Dolphin, D., Ed. (1978) *The Porphyrins*, Vol. 1, Academic Press, New York.

Gelin, B. R., Lee, A. W., & Karplus, M. (1983) *J. Mol. Biol. 171*, 489.

Gibson, Q. H., & Antonini, E. (1963) *J. Biol. Chem. 283*, 1384–1388.

Ho, C., & Russu, I. M. (1981) *Methods Enzymol. 76*, 275–312.

Imai, K. (1985) *Acta Haematol. Jpn. 48*, 317–325.

Ishimori, K., & Morishima, I. (1986) *Biochemistry 25*, 4892–4898.

Kawabe, K., Imaizumi, K., Imai, K., Tyuma, I., Ogoshi, H., Iwahara, T., & Yoshida, Z.-1. (1982) *J. Biochem. 92*, 1713–1722.

Kitagawa, T. (1986) *Adv. Spectrosc. (Chichester, U.K.) 13*, 443–481.

Kitagawa, T., Nagai, K., & Tsubaki, M. (1979), *Febs. Lett. 104*, 376–378.

LaMar, G. N. (1979) in *Biological Applications of Magnetic Resonance* (Shulman, R. G., Ed.) pp 305–343, Academic Press, New York.

Lee, H., Kitagawa, T., Abe, M., Pandey, R. K., Leung, H.-K., & Smith, K. M. (1986) *J. Mol. Struct. 146*, 329–347.

Li, X.-Y., Czernuszewicz, R. S., Kincaid, J. R., & Spiro, T. G. (1989) *J. Am. Chem. Soc. 111*, 7012–7035.

Makino, N., & Sugita, Y. (1978) *J. Biol. Chem. 253*, 1174–1178.

Matsukawa, S., Mawatari, K., Yoneyama, Y., & Kitagawa, T. (1985) *J. Am. Chem. Soc. 107*, 1108–1113.

Nagai, K., & Kitagawa, T. (1980) *Proc. Natl. Acad. Sci. U.S.A. 77*, 2033–2037.

Nagai, K., Kitagawa, T., & Morimoto, H. (1980) *J. Mol. Biol. 136*, 271–289.

Nagai, K., Lamar, G. N., Jue, T., & Bunn, H. F. (1982) *Biochemistry 21*, 842.

Ondrias, M. R., Rousseau, D. L., Kitagawa, T., Ikeda-Saito, M., Inubushi, T., & Yonetoni, T. (1982) *J. Biol. Chem. 257*, 8766–8770.

Perutz, M. F., Fermi, G., Luisi, B., Shannan, B. S., & Liddington, R. C. (1987) *Acc. Chem. Res. 20*, 309.

Pettigrew, D. W., Romeo, P. H., Tsapais, A., Thillet, J., Smith, M. L., Turner, B. W., & Ackers, G. K. (1982) *Proc. Natl. Acad. Sci. U.S.A. 79*, 1849–1853.

Riggs, A. (1981) *Methods Enzymol. 76*, 5–29.

Rosseau, D. L., & Friedman, J. M. (1988) *Biological Applications of Raman Spectroscopy*, Vol. 3, pp 133–215, Wiley, New York.

Rossi-Fanelli, A., Antonini, E., & Caputo, A. (1959) *Arch. Biochem. Biophys. 85*, 37–42.

Rousseau, D. L., & Ondrias, M. R. (1983) *Annu. Rev. Biophys. Bioeng. 12*, 357–380.

Seybert, D. W., Moffat, K., & Gibson, Q. H. (1976) *J. Biol. Chem. 251*, 45–52.

Simolo, K., Stucky, G., Chen, S., Bailey, M., Scholes, C., & McLendon, G. (1985) *J. Am. Chem. Soc. 107*, 2865-2872.
Smith, K. M., Ed. (1975) *Porphyrins and Metalloprophyrins*, p 804.9, Elsevier, Amsterdam.
Sono, M., & Asakura, T. (1974) *J. Biol. Chem. 249*, 7087-7093.
Spiro, T. G. (1985) *Adv. Protein Chem. 37*, 111.
Srajer, V., Reinisch, L., & Champion, P. M. (1988) *J. Am. Chem. Soc. 110*, 6656-6670.
Sugita, Y. (1975) *J. Biol. Chem. 250*, 1251-1256.
Uchida, K., Yuko, S., Hirotani, E., Kimura, K., Yoneyama, T., Takenchi, H., & Harada, I. (1988) *J. Biochem. 103*, 979-985.
Yammamoto, H., & Yonetani, T. (1974) *J. Biol. Chem. 249*, 7964-7968.
Yip, Y. K., Waks, M., & Beychok, S. (1972) *J. Biol. Chem. 247*, 7237-7244.
Yip, Y. K., Waks, M., & Beychok, S. (1977) *Proc. Natl. Acad. Sci. U.S.A. 74*, 64-68.
Yu, N. T. (1986) *Methods Enzymol. 130*, 350-409.

Effect of Phosphatidylethanolamine on the Properties of Phospholipid-Apolipoprotein Complexes†

Elizabeth A. Bonomo* and John B. Swaney
Department of Biological Chemistry, Hahnemann University, Philadelphia, Pennsylvania 19102
Received April 4, 1989; Revised Manuscript Received January 9, 1990

ABSTRACT: Plasma high density lipoproteins (HDL) are synthesized in intestinal mucosal cells and hepatocytes and are secreted into the blood. Factors influencing the structure and function of these HDL, such as lipid and protein composition, are poorly understood. It appears, however, that intracellular, discoidal HDL are enriched, relative to plasma HDL, in phosphatidylethanolamine (PE), a phospholipid known to generate unusual, nonbilayer structures of putative physiological significance. Although incubation of dimyristoylphosphatidylcholine (DMPC) with apolipoprotein A-I at the gel–liquid crystalline phase transition temperature results in the spontaneous formation of lipid–protein complexes, the presence of proportionately small amounts of PE prevents the formation of such complexes, suggesting that PE profoundly alters the phase properties of the phospholipid bilayers. However, by using a detergent-mediated method for the formation of PE-rich model nascent HDL from phospholipids and apolipoprotein A-I, lipid–protein complexes containing as much as 75% DLPE could be formed, thus demonstrating that the presence of PE causes a kinetic, rather than a thermodynamic, barrier to spontaneous complex formation. The products contained a DLPE:DMPC molar ratio similar to that of the initial incubation mixture; however, as the mole percentage of DLPE increased, the products became less heterogeneous, the buoyant density of the products increased, and the Stokes diameter of the products decreased. Similar results were obtained when dimyristoylphosphatidylethanolamine (DMPE) and dipalmitoylphosphatidylethanolamine (DPPE) were employed in lieu of DLPE. Electron microscopy of complexes containing DLPE and DMPC at a 1:1 molar ratio showed that these particles possessed a discoidal, bilayer morphology similar to that seen with complexes containing only phosphatidylcholine. PE increased the susceptibility of the particles to denaturation by guanidine hydrochloride and caused a much sharper endotherm at the phase transition as shown by differential scanning calorimetry; however, circular dichroism studies showed that the A-I secondary structure was similar in complexes with DMPC alone and when complexed with a mixture of DMPC and DLPE. The results from these experiments suggest that the presence of DLPE in a mixture with DMPC diminishes the interaction between protein and lipid in these complexes. We conclude that under appropriate conditions, phosphatidylethanolamines can be incorporated into model nascent HDL, but the presence of PE significantly alters certain of the physical properties of these HDL, such as size and density, compared to those prepared with phosphatidylcholines alone.

Plasma lipoproteins are soluble, pseudomicellar, lipid–protein assemblies that transport lipids to and from tissues and mediate several reactions of lipid metabolism. Plasma high density lipoproteins (HDL)[1] are spherical particles with a diameter range of 8.5–12.0 nm (Anderson et al., 1977). Human plasma HDL are composed of a neutral lipid apolar core consisting of cholesteryl ester and triglyceride that is solubilized by an outer surface of amphoteric lipids and apolipoproteins A-I, A-II, and C. Transitory precursors of plasma HDL, termed nascent HDL, appear to be secreted in three discrete forms: as phospholipid-rich, discoidal structures, as phospholipid-rich, small, spherical structures, and as free apolipoproteins not bound to lipid (Marsh, 1976; Hamilton et al., 1976; Bisgaier

†This research was supported by Research Grant HL 33827 from the National Institutes of Health. E.A.B. was a Predoctoral Fellow of the Southeastern Pennsylvania Affiliate of the American Heart Association.
*Address correspondence to this author at the Department of Chemistry, Philadelphia College of Pharmacy and Science, Philadelphia, PA 19104.

[1] Abbreviations: HDL, high density lipoproteins; apo A-I, apolipoprotein A-I; PC, phosphatidylcholine; PE, phosphatidylethanolamine; DPPC, dipalmitoylphosphatidylcholine; DMPC, dimyristoylphosphatidylcholine; DLPE, dilauroylphosphatidylethanolamine; DMPE, dimyristoylphosphatidylethanolamine; DPPE, dipalmitoylphosphatidylethanolamine; A-I, apolipoprotein A-I; GGE, pore limit gradient gel electrophoresis; DMS, dimethyl suberimidate; SDS-PAGE, polyacrylamide gel electrophoresis in sodium dodecyl sulfate; LCAT, lecithin: cholesterol acyltransferase.

0006-2960/90/0429-5094$02.50/0